

Multichannel Penning detachment of H^- from excited Li and Ca atoms

F. Martín* and R. S. Berry

Department of Chemistry and The James Franck Institute, The University of Chicago, 5735 South Ellis Avenue, Chicago, Illinois 60637-1403

(Received 21 January)

We develop theoretical cross sections for Penning detachment of H^- from excited Li and Ca atoms for impact energies between 25 meV and 20 eV. We examine two kinds of cases: those that leave the target in its ground state and those that leave the target excited after the collision, namely, $H^- + Li(3s)$, $H^- + Li(3p)$, $H^- + Li(3d)$, and $H^- + Ca(4s5s^1S^e)$. Our results show that, in general, Penning detachment is enhanced when several decay channels are open and that the target is left preferentially in the nearest excited state. [S1050-2947(97)00506-4]

PACS number(s): 34.50.Fa

I. INTRODUCTION

Penning detachment is the name we have given to the process in which a negative ion A^- collides with an electronically excited energy donor N^* and the energy of excitation passes from the donor to the negative ion and sets the excess electron free, leaving as final products $A + N + e^-$. The process was so named by analogy with Penning ionization, the well-studied collision process $A + N^* \rightarrow A + N^+ + e^-$. Typical cross sections for Penning ionization are roughly like gas-kinetic cross sections, of order 10^{-16} cm^2 [1,2]. Cross sections for simple collisional detachment can be much smaller (see, e.g., [3] and references therein) because their magnitudes come largely from crossing-point interactions of potential-energy curves for bound and free states of the *extra* electron. By contrast, early estimates [4] of the cross sections for Penning detachment indicated that these should be considerably larger than either of these, possibly even of the order 10^{-14} cm^2 . Hence the process is tantalizing for study, even for this reason alone. Cross sections this large imply that Penning detachment must play an important role in kinetics of almost any gaseous or plasma environment in which negative ions and excited atoms or molecules are both present. Nevertheless, it has gone nearly unstudied until now [5,6].

In a previous work [7] we have studied Penning detachment of H^- by impact of excited He and Li atoms. In that paper, we considered Penning detachment processes in which the neutral atom remains in the ground state. This led us to understand the basic principles that govern Penning detachment and to provide total cross sections for collisions in which the target is initially in the lowest excited state: $H^- + Li^*(1s^22p)$ and $H^- + He^*(1s2s^1S^e)$. In these cases all the excitation energy is used to detach the excess electron from the ion. In contrast, when the target is initially in a higher excited state, the excitation energy may be large enough to detach an electron and leave the target in a lower excited state. For example, in the collision $H^- + Li^*(1s^23s)$, the Li atom can be left in either the ground state $Li(1s^22s)$ or the first excited state $Li^*(1s^22p)$. Al-

though in [7] we also investigated detachment from $Li^*(1s^23s)$, $Li^*(1s^23p)$, and $Li^*(1s^23d)$ excited states, we only allowed for decay into the ground state of Li, so that the computed cross sections do not correspond to total cross sections.

In this work we study multichannel Penning detachment processes by considering all energetically allowed final states of the target. Our aim is not only to provide total Penning detachment cross sections for these cases but also to find out how the presence of several open channels affects this process, either by enhancing its cross section or by redistributing the products among the accessible final states. This may be valuable information for experiments in progress [8] because, although single-channel Penning detachment cross sections are very large, the available ion densities are rather small. Since experiments carried out in our laboratory make use of Ca atoms as energy donors, we will also present calculations for Penning detachment of H^- from excited Ca. As is well known, electron correlation between the two valence electrons of Ca is very important [9], which is a major difference from the targets investigated in [7]. Thus our calculations with Ca targets will also allow us to study the role of initial-state correlation in the process.

In the next section we briefly describe the methods used to carry out the calculations. Section III presents the cross sections and Sec. IV a discussion of the results and their implications. Atomic units are used throughout unless otherwise stated.

II. THEORETICAL METHOD

A. Local approximation

We treat the problem semiclassically in this sense: the nuclei follow classical trajectories in the field induced by the effective interatomic potential, whereas the electrons are described quantum mechanically. On any given nuclear trajectory, the electronic wave function is the solution of the Schrödinger equation

$$i \frac{d}{dt} \Psi(t) = \mathcal{H}_{el} \Psi(t), \quad (1)$$

where \mathcal{H}_{el} is the molecular Born-Oppenheimer Hamiltonian, which depends parametrically on time through the internu-

*Permanent address: Departamento de Química C-9, Universidad Autónoma de Madrid, 28049 Madrid, Spain.

clear distance $R(t)$, $\Psi(t)$ is the electronic wave function, and t is the time coordinate of the collision event. The initial state of the system, $A^- + N^*$, is embedded in the electronic continuum of the molecular negative ion AN^- formed during the collision. With this picture in mind, we define a basis of states as follows. Bound electronic states for $t = -\infty$ are formally the solutions of

$$(Q\mathcal{H}_{\text{el}}Q - E_i)\psi_i = 0 \quad (2)$$

and (unbound) electronic continuum states are the solutions of

$$(P_{\nu l}\mathcal{H}_{\text{el}}P_{\nu l} - E)\psi_{E,\nu l} = 0, \quad (3)$$

where ν represents the set of quantum numbers describing the final state of the target, l is the angular momentum of the ejected electron, and $P_{\nu l}$ and Q are projection operators that satisfy the exclusionary conditions

$$P_{\nu l}P_{\nu' l'} = \delta_{\nu\nu'}\delta_{ll'}, \quad (4)$$

$$P = \sum_{\nu} \sum_l P_{\nu l}, \quad (5)$$

$$PQ = 0, \quad (6)$$

$$P + Q = 1 \quad (7)$$

for all R .

To solve Eq. (1) in [7] we used the close-coupling method by expanding the electronic wave function $\Psi(t)$ in the basis $\{\psi_i, \psi_{E,\nu l}\}$. An explicit solution of the corresponding system of coupled equations showed that, for collision velocities smaller than 0.01 a.u., all dynamical couplings corresponding to the breakdown of the Born-Oppenheimer approximations can be neglected. The calculations also showed that the couplings $\langle \psi_{E,\nu l} | P_{\nu l} \mathcal{H}_{\text{el}} P_{\nu' l'} | \psi_{E,\nu' l'} \rangle$ are responsible for a redistribution of the population within the continuum and barely contribute to the total detachment process, which is mainly controlled by the bound-continuum couplings $\langle \psi_i | Q \mathcal{H}_{\text{el}} P_{\nu l} | \psi_{E,\nu l} \rangle$. Finally, we found that, under these conditions, a local approximation [10,11], which assumes that the entrance channel ψ_0 is well separated in energy from the remaining Q states and that the resonant state formed in the collision decays exponentially, leads to Penning detachment cross sections that are almost identical to those obtained with the much more involved close-coupling method. For this reason, and since the number of continuum states one must include in a multichannel problem is much larger than in [7], we use the local approximation to evaluate the total Penning detachment cross sections in this work. In this approximation, the total ionization probability for a given nuclear trajectory can be written

$$P(b) = 1 - \exp\left(-2 \int_{R_0}^{\infty} \Gamma(R)/v(R) dR\right), \quad (8)$$

where $\Gamma(R)$ is the total width of the ψ_0 state

$$\Gamma(R) = 2\pi \sum_{\nu} \sum_l |\langle \psi_0 | Q \mathcal{H}_{\text{el}} P_{\nu l} | \psi_{E=E_0,\nu l} \rangle|^2, \quad (9)$$

$v(R)$ is the radial velocity of the nuclei

$$v(R) = \frac{1}{v_0 \sqrt{1 - \frac{2V(R)}{\mu v_0^2} - \frac{b^2}{R^2}}}, \quad (10)$$

and R_0 is the classical turning point. $V(R)$ is the interatomic potential, μ the reduced mass of the nuclei, v_0 the initial velocity, and b the impact parameter. The total detachment cross section is given by

$$\sigma = 2\pi \int_0^{\infty} b P(b) db. \quad (11)$$

B. Wave functions

In the $H^- + Li^*$ collision, Penning detachment is essentially a two-electron process in which the energy of the excited electron of Li is transferred to the loosely bound electron of H^- , the other electrons remaining passive during the collision. Therefore, the dynamics of the Penning detachment process can be studied using an effective two-electron Hamiltonian \mathcal{H}_{el} . In the $H^- + Li^*$ case we have used the same model Hamiltonian and the same Q wave functions as in [7]. Besides the P functions used in [7] to describe the final continuum states associated with the lowest target state $Li(2s)$, in this work we have also included those associated to the first excited state $Li(2p)$. In the latter case, the two-electron continuum states are built using the same discretized continuum orbitals of H^- as those used in [7] for the former case.

For the $H^- + Ca^*$ collision, the situation is more complicated because the electron correlation between the two valence electrons of calcium cannot be neglected. So one has to extend the techniques developed in [7] to deal with an effective three-electron system. The potentials that describe the interaction between an electron and the core of the negative ion and between an electron and the Ca core (i.e., an electron and a Ca^{2+} ion) take the simple forms [12,13]

$$V_{H^-} = -\frac{Z_{H^-}}{r_{H^-}} (1 + \alpha_{H^-} r_{H^-}) e^{-2\alpha_{H^-} r_{H^-}}, \quad (12)$$

$$V_{Ca} = -\frac{1}{r_{Ca}} - \frac{(Z_{Ca} - 1)}{r_{Ca}} (1 + \alpha_{Ca} r_{Ca}) e^{-2\alpha_{Ca} r_{Ca}}, \quad (13)$$

whose analytic expressions are identical to those used in [7]. As in the latter work, we use $\alpha_{H^-} = 0.6973$. For the Ca potential we have used $\alpha_{Ca} = 1.7228$. The effective three-electron Hamiltonian is written

$$\mathcal{H}_{\text{el}} = \mathcal{H}_{H^-(1)} + \mathcal{H}_{Ca(2,3)} + V_{H^-(2)} + V_{H^-(3)} + V_{Ca(1)} + \frac{1}{r_{12}} + \frac{1}{r_{13}}, \quad (14)$$

where

$$\mathcal{H}_{H^-(1)} = -\frac{1}{2} \nabla_1^2 + V_{H^-(1)} \quad (15)$$

and \mathcal{H}_{Ca} is an effective two-electron Hamiltonian for the Ca atom:

$$\mathcal{H}_{Ca}(2,3) = -\frac{1}{2}\nabla_2^2 - \frac{1}{2}\nabla_3^2 + V_{Ca}(2) + V_{Ca}(3) + \frac{1}{r_{23}}. \quad (16)$$

The latter Hamiltonian includes neither valence-core polarization potentials nor dielectronic polarization potentials that are essential to obtain highly accurate energy levels [14]. However, our aim is not to reach spectroscopic accuracy for the Ca atomic states, but to provide a basis of correlated Ca states for the dynamical treatment; we do not expect these terms to have a significant effect in the calculated cross sections.

The Q states are obtained by diagonalizing $Q\mathcal{H}_{el}Q$ in a basis of (properly antisymmetrized) three-electron configurations of the form $\{\varphi_{1sH^-}\Phi_{kCa}\}$, where φ_{1sH^-} is the lowest one-electron orbital of the anion and the Φ_{kCa} functions are the eigenstates of the calcium Hamiltonian \mathcal{H}_{Ca} . The Φ_{kCa} states included in the present calculations are $1S^e(4s^2)$, $1D^e(4s3d)$, $1P^o(4s4p)$, $1S^e(4s5s)$, $1D^o(4p3d)$, $1D^e(4s4d)$, $1P^o(4s5p)$, $1F^o(4p3d)$, $1S^e(4s6s)$, $1P^o(4s6p)$, and $1D^e(4s5d)$. Configurations with three active electrons in Ca (i.e., corresponding to the Ca^- ion) are not included in the diagonalization procedure since their contribution to the Penning detachment process is expected to be small. The Ca states are obtained by diagonalizing \mathcal{H}_{Ca} in a basis of properly antisymmetrized two-electron configurations of the form $\varphi_{iCa}\varphi_{jCa}$, where the φ_{iCa} functions are the eigenfunctions of the Ca^+ Hamiltonian

$$\left(-\frac{1}{2}\nabla^2 + V_{Ca}\right)\varphi_{iCa} = \epsilon_{iCa}\varphi_{iCa}. \quad (17)$$

All φ orbitals are written as linear superpositions of Gaussian-type orbitals (GTOs). An illustration of the quality of our description for the Ca states is provided by the calculated value of the ground-state polarizability, which is 174 a.u., to be compared with the experimental value of 169 ± 17 a.u. [15]. To avoid any possible inconsistency in the evaluation of the cross sections, we have used the experimental energies of calcium [16] at $R=\infty$.

The P states are (properly antisymmetrized) three-electron configurations of the form $\tilde{\psi}_{E,vl} = \tilde{\varphi}_{\epsilon,l}\Phi_{\nu Ca}$, where $\Phi_{\nu Ca}$ is the final two-electron state of Ca and the $\tilde{\varphi}_{\epsilon,l}$ functions are discretized continuum orbitals. We have evaluated these states for all accessible $\Phi_{\nu Ca}$ states of calcium. The discretized continuum orbitals $\tilde{\varphi}_{\epsilon,l}$ are obtained by diagonalizing the one-electron Hamiltonian \mathcal{H}_{H^-} using an even-tempered sequence of GTOs for each l [17] and correspond to those solutions with energies lying above the detachment threshold of H^- . The discretized electronic continuum thus obtained is handled as in [7]. Only $l=0$ and $l=1$ continuum states have been included since, as explained in [7], higher angular momenta lead to a redistribution of the final state population but barely affect the value of the total cross section.

III. RESULTS

A. $H^- + Li^*$

In Fig. 1 we show the energy correlation diagram for the Q states of the LiH^- quasimolecule. As explained in [7], the

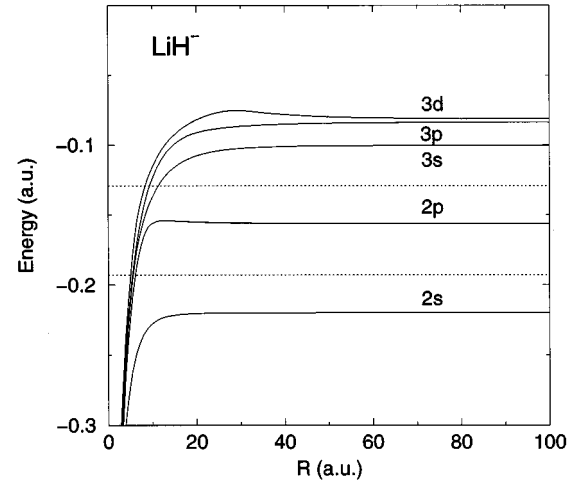


FIG. 1. Potential-energy curves for the LiH^- quasimolecule. The labels nl represent the asymptotic states $H^- + Li(1s^2nl)$. The dotted lines show the position of the ionization thresholds $H^- + Li(1s^22s) + e^-$ and $H^- + Li(1s^22p) + e^-$.

calculated potential-energy curves should be reliable for $R > 2$ a.u. where delocalization effects that might affect the inner atomic cores are negligible. Figure 1 also shows the position of the two lowest detachment thresholds. It can be seen that the Q states dissociating into $H^- + Li(3s)$, $H^- + Li(3p)$, and $H^- + Li(3d)$ can decay either to $H + Li(2s) + e^-$ or $H + Li(2p) + e^-$, whereas the Q state dissociating into $H^- + Li(2p)$ can decay only to $H + Li(2s) + e^-$. The total Penning detachment cross sections for the former three cases are given in Fig. 2. It can be observed that the values of these cross sections in the high-energy region are at least twice as large as the ones reported in [7] where decay to $H + Li(2p) + e^-$ was not included. At lower energies, the present values are closer to the ones reported previously because the Penning detachment process is almost entirely dominated by nuclear trajectory effects: the Langevin effect [18] in the case of $H^- + Li(3s)$ [and to a lesser extent $H^- + Li(3p)$], and the potential barrier that shuts off Penning detachment in

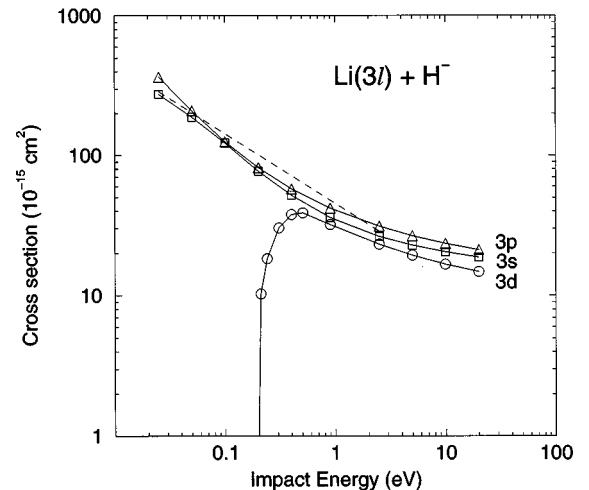


FIG. 2. Total Penning detachment cross sections for the $H^- + Li(3s)$, $H^- + Li(3p)$, and $H^- + Li(3d)$ collisions. The dashed line is the Langevin approximation.

the case of $\text{H}^- + \text{Li}(3d)$. As explained in [7], the Langevin model assumes that the transition probability is equal to one for impact parameters smaller than that for which the projectile orbits about the target. Consequently, in this model the cross section is independent of the nature of the couplings and is determined completely by the polarizability α of the initial target state through the formula [18]

$$\sigma = \frac{2\pi}{v_0} \left(\frac{\alpha}{\mu} \right)^{1/2}. \quad (18)$$

The dashed line in Fig. 2 shows the results obtained from this equation.

As the local approximation neglects coherence between open channels, it is not possible to know from this approximation how much is left in the individual channels $\text{Li}(2s)$ and $\text{Li}(2p)$. However, it is still possible to infer whether transitions to each channel are equally important or, by contrast, one channel dominates the detachment process. To answer this question, we have also performed calculations by closing artificially the lowest detachment channel $\text{H} + \text{Li}(2s) + e^-$. The results so obtained are very close to those shown in Fig. 2, thus indicating that, in a first step, the dominant process is the transition from the initial state to the continuum associated with the highest available channel. One might be tempted to say that this is not surprising for the $\text{Li}(3s)$ and $\text{Li}(3d)$ initial states because dipolar decay to $\text{Li}(2p)$ is highly probable, but it is rather unexpected for $\text{Li}(3p)$ because the latter might be expected to decay mainly to $\text{Li}(2s)$. However, this argument does not take into account that all these states suffer from Stark mixing, so that all of them have a component that can decay to $\text{Li}(2p)$ through a dipolar transition. In fact, we have shown in [7] that Stark mixing for the $n=3$ states of Li takes place at distances as large as 100 a.u., so that the $\text{Li}(3p)$ state may undergo an effective dipolar transition to $\text{Li}(2p)$. Then, from these calculations, we can conclude that, as far as dipolar decay of the initial state is possible, the collision leaves the neutral atom in the closest excited states, so that the ejected electrons have the lowest possible kinetic energy. The $\text{H} + \text{Li}(2p) + e^-$ channel may be populated in a second step as a result of the interaction with the $\text{H} + \text{Li}(2s) + e^-$ channel.

B. $\text{H}^- + \text{Ca}^*$

In Fig. 3 we show the energy correlation diagram for the Q states of the CaH^- quasimolecule. The figure also shows the position of the three lowest detachment thresholds. As in the previous case, we expect our calculated potential-energy curves to be reliable for $R > 2$ a.u. In this case we have studied Penning detachment of H^- from the three lowest excited states of calcium: ${}^1D^e(4s3d)$, ${}^1P^o(4s4p)$, and ${}^1S^e(4s5s)$. Penning detachment of H^- from the two former states can leave Ca only in its ground state ${}^1S^e(4s^2)$, whereas Penning detachment from the latter state can leave Ca in either the ground state or the ${}^1D^e(4s3d)$ or ${}^1P^o(4s4p)$ excited state (see Fig. 3). The corresponding total Penning detachment cross sections are presented in Fig. 4. We have not considered detachment from more excited states of calcium because the number of open channels in-

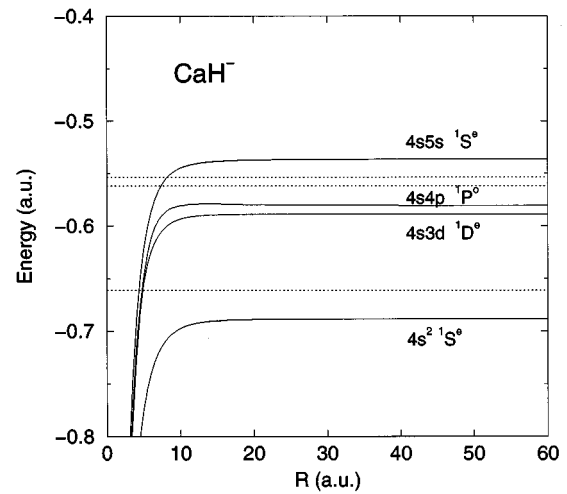


FIG. 3. Potential-energy curves for the CaH^- quasimolecule. The labels $nl n' l'$ represent the asymptotic states $\text{H}^- + \text{Ca}(nl n' l')$. The dotted lines show the position of the ionization thresholds $\text{H} + \text{Ca}(4s^2 1S^e) + e^-$, $\text{H} + \text{Ca}(4s3d 1D^e) + e^-$, and $\text{H} + \text{Ca}(4s4p 1P^o) + e^-$.

creases substantially when we go up in energy, thus complicating the theoretical calculations.

We discuss first detachment from the two lowest excited states that can decay only to the ground state of Ca. Figure 4 shows that the cross sections for these two processes are very similar in the higher-energy region. In fact, the ${}^1D^e(4s3d)$ and ${}^1P^o(4s4p)$ states are so close in energy (see Fig. 3) that mixing induced by the H^- ion is important even at very long internuclear distances. Consequently, both states have a comparable P component that can decay to the S ground state through a dipolar transition. The different behavior observed at very low energies results from the differences in the interatomic potentials: while the potential-energy curve of the quasimolecular state dissociating into $\text{H}^- + \text{Ca}(4s3d 1D^e)$ is attractive in the region of physical interest, that of the state dissociating into H^-

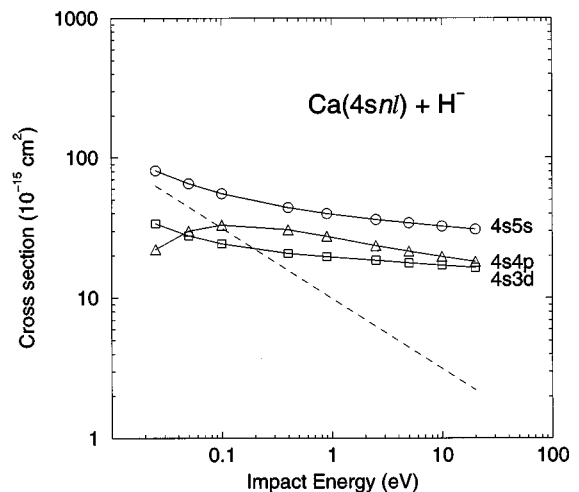


FIG. 4. Total Penning detachment cross sections for the $\text{H}^- + \text{Ca}(4s3d 1D^e)$, $\text{H}^- + \text{Ca}(4s4p 1P^o)$, and $\text{H}^- + \text{Ca}(4s5s 1S^e)$ collisions. The dashed line is the Langevin approximation.

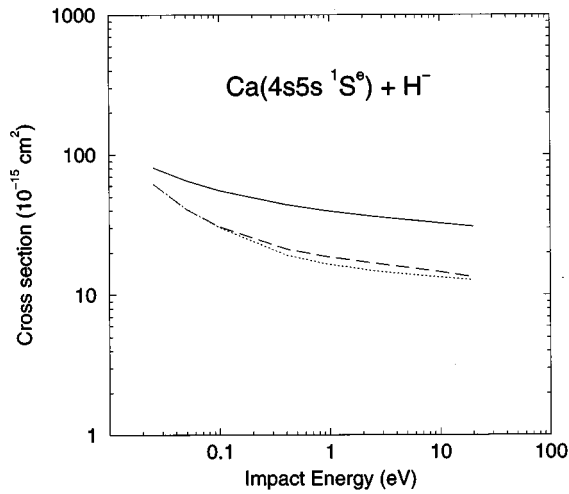


FIG. 5. Penning detachment cross sections for the $H^- + Ca(4s5s\ ^1S^e)$ collision obtained by closing the $H + Ca(4s^2\ ^1S^e) + e^-$ and $H + Ca(4s3d\ ^1D^e) + e^-$ channels (full line), by closing the $H + Ca(4s3d\ ^1D^e) + e^-$ and $H + Ca(4s4p\ ^1P^o) + e^-$ channels (dashed line), and by closing the $H + Ca(4s^2\ ^1S^e) + e^-$ and $H + Ca(4s4p\ ^1P^o) + e^-$ channels (dotted line).

$+Ca(4s4p\ ^1P^o)$ is slightly repulsive. Therefore, at very low impact energies, Penning detachment from $Ca(4s4p\ ^1P^o)$ is hindered and the cross section decreases. In any case, the curves shown in Fig. 4 are rather flat in the region of impact energies considered in this work because the cross sections are so large at high energies that trajectory effects do not play a significant role in this case. [We found a similar situation in [7] for the collision $H^- + Li(2p)$.]

As mentioned above, Penning detachment from $Ca(4s5s\ ^1S^e)$ can also leave Ca in an excited state. It can be observed in Fig. 4 that at very low impact energies the cross section tends to the Langevin values. The explanation for this behavior is the same as the one given in Sec. III A. However, in the present case, the actual cross section is much larger than the Langevin cross section (especially at higher energies), so that the Langevin effect is less apparent. As in Sec. III A, we can get significant physical insight into the roles of the different detachment channels by closing artificially some of them. In Fig. 5 we present results obtained by closing two channels, so that Penning detachment is only possible to the remaining channel. It can be seen that the dominant process is $H^- + Ca(4s5s\ ^1S^e) \rightarrow H + Ca(4s4p\ ^1P^o) + e^-$. Moreover, the corresponding cross section is almost identical to the one obtained by including all three channels. Therefore, as in the case of excited Li atoms, Penning detachment takes place through the nearest excited state of the target. Besides, it corresponds to the allowed dipolar transition $Ca(4s5s\ ^1S^e) \rightarrow Ca(4s4p\ ^1P^o)$, which explains the high value of the cross section. Again we observe that Penning detachment is enhanced with respect to those cases for which only one decay channel is available.

IV. CONCLUSION

We have studied Penning detachment of H^- from excited Li and Ca atoms for impact energies between 25 meV and 20

eV. We have focused on those cases for which the excitation energy of the donor is large enough to leave it in an excited state, namely, $H^- + Li(3s)$, $H^- + Li(3p)$, $H^- + Li(3d)$ and $H^- + Ca(4s5s\ ^1S^e)$. Our results show that Penning detachment is enhanced when several decay channels are open. In the case of Li projectiles with excited electrons in the $n=3$ shell, Penning detachment proceeds through the excited $Li(2p)$ state, thus yielding electrons with the lowest possible energy. In the case of $Ca(4s5s\ ^1S^e)$, the dominant process is decay to the neighboring $Ca(4s4p\ ^1P^o)$ state. We can then conclude that the dominant mechanism is a transition from the initially bound state to the continuum states associated with the nearest detachment threshold. The remaining open channels may be populated as well, but likely as the result of a second transition from the dominant detachment channel (direct transitions from the entrance channel are expected to be important only at short internuclear distances, so that their relative contribution to the total cross section is less significant).

In particular, our calculations for excited Ca targets lead to cross sections that are larger than 10^{-14} cm^2 across the whole energy range investigated here. This result is in reasonable agreement with order-of-magnitude estimates obtained from recent experiments using Ca atoms as energy donors and O^- anions [8].

Finally, our results for Ca targets show that, although electron correlation is extremely important to describe properly the initial and final states of calcium, it does not seem to introduce new variables in our understanding of Penning detachment processes. Indeed, Penning detachment is the result of the interaction between target and projectile electrons. Since this interaction leads to detachment at rather long internuclear distances, one can expect that target electron correlation is only needed to account properly for Stark mixing induced by the charged projectile. Provided that this requirement is fulfilled, the basic mechanisms responsible for Penning detachment are essentially the same as in the case of effective one-electron targets.

Thus far, we have investigated only processes whose final channel corresponds to free states of two neutral atoms and an electron. Whether directly or by exchange, the departing electron in effect leaves the negative ion. A second kind of channel is possible if either the neutral atom is very highly excited or the atoms remain in a molecular bound vibrational state: this is the process in which the atoms form an ion pair N^+A^- in the final state. The free channel with these products is not available for the processes considered here. In future work, we plan to address the associative process, which may be important in collisions of alkali- and alkaline-earth atoms with H^- and halide ions.

ACKNOWLEDGMENTS

This research was supported by a Grant from the National Science Foundation. F.M. would like to acknowledge the support of the Ministerio de Educación y Ciencia (Programa de Movilidad Temporal de Personal Funcionario, Docente e Investigador No. PR95-235) for a sabbatical leave at the University of Chicago.

- [1] R.S. Berry, in *Advances Electronics and Electron Physics*, edited by L. Marton and C. Marton (Academic, New York, 1980), p. 137.
- [2] P.E. Siska, *Rev. Mod. Phys.* **65**, 337 (1993).
- [3] Y. Wang, R.L. Champion, and L.D. Doverspike, *Phys. Rev. A* **35**, 1503 (1987).
- [4] B. Blaney and R.S. Berry, *Phys. Rev. A* **3**, 1349 (1971).
- [5] F.C. Fehsenfeld, D. Albritton, J.A. Burt, and H.I. Schiff, *Canad. J. Chem.* **47**, 1793 (1969).
- [6] D. Doweck, J.C. Houver, J. Pommier, C. Richter, T. Royer, and N. Andersen, in *Proceedings of the XVIth International Conference on the Physics of Electronic and Atomic Collisions*, edited by Alexander Dalgarno (North-Holland, Amsterdam, 1989), p. 501.
- [7] F. Martín and R.S. Berry, *Phys. Rev. A* (to be published).
- [8] S. Darveau, R. Niedziela, B. Prutzman, Z. Herman, and R.S. Berry (unpublished).
- [9] J.E. Hunter III and R.S. Berry, *Phys. Rev. Lett.* **59**, 2959 (1987).
- [10] K. Katsuura, *J. Chem. Phys.* **42**, 3771 (1965).
- [11] R. D. Taylor and J. B. Delos, *Proc. R. Soc. London Ser. A* **379**, 179 (1982).
- [12] Y.D. Wang, C.D. Lin, N. Toshima, and Z. Chen, *Phys. Rev. A* **52**, 2852 (1995).
- [13] H. Bachau, P. Galan, F. Martín, A. Riera, and M. Yáñez, *At. Data Nucl. Data Tables* **44**, 305 (1990).
- [14] C. Laughlin and J.E. Hansen, *J. Phys. B* **29**, L441 (1996).
- [15] T.M. Miller and B. Bederson, *Phys. Rev. A* **14**, 1572 (1976).
- [16] S. Bashkin and J.O. Stoner, Jr., *Atomic Energy Levels and Grotrian Diagrams* (Elsevier, New York, 1975).
- [17] A. Macías, F. Martín, A. Riera, and M. Yáñez, *Phys. Rev. A* **36**, 4179 (1987).
- [18] P. Langevin, *Ann. Chim. Phys.* **5**, 245 (1905); E.W. McDaniel, *Collision Phenomena in Ionized Gases*(Wiley, New York, 1964).